Disorder-Induced Strongly Correlated Photons in Waveguide QED

Guoqing Tian,[1] Li-Li Zheng,[2,*] Zhi-Ming Zhan,[2] Franco Nori,[3,4] and Xin-You Lü[1,†]
[1]School of Physics and Institute for Quantum Science and Engineering, Huazhong University of Science and Technology, and Wuhan Institute of Quantum Technology, Wuhan, 430074, China
[2]School of Artificial Intelligence, Jianghan University, Wuhan 430074, China
[3]Quantum Computing Center, RIKEN, Wakoshi, Saitama 351-0198, Japan
[4]Department of Physics, University of Michigan, Ann Arbor, Michigan 48109-1040, USA

(Received 14 April 2025; accepted 9 September 2025; published 9 October 2025)

Strongly correlated photons play a crucial role in modern quantum technologies. Here, we investigate the probability of generating strongly correlated photons in a chain of N qubits coupled to a one-dimensional waveguide. We found that disorder in the transition frequencies can induce photon antibunching and especially nearly perfect photon blockade events in the transmission and reflection outputs. As a comparison, in ordered chains, strongly correlated photons cannot be generated in the transmission output, and only weakly antibunched photons are found in the reflection output. The occurrence of nearly perfect photon blockade events stems from the disorder-induced nearly completely destructive interference of photon scattering paths. Our Letter highlights the impact of disorder on photon correlation generation and suggests that disorder can enhance the potential for achieving strongly correlated photons.

DOI: 10.1103/mldt-d59t

Strongly correlated photons are of importance in a wide range of quantum optical applications, including quantum communication [1–3], quantum computation [4–6], and the study of fundamental quantum mechanics [7,8]. Various methods have been developed to produce such strongly correlated photons in the fields of cavity QED [9–12] and waveguide QED [13–15]. In particular, the one-dimensional (1D) waveguide QED platform offers a highly controlled environment for interacting photons with quantum emitters, providing an excellent means to realize strongly correlated photons [16–20]. By leveraging the properties of waveguide structures and the coupling with quantum emitters, the scattered light can exhibit either temporal photon attraction (bunching) or repulsion (antibunching), owing to the interference effects and the intrinsic nonlinearity of quantum emitters, making the waveguide QED platform stand out as a powerful tool for generating and manipulating strongly correlated photons for quantum technologies [21–28].

In practical experimental settings, disorder arising from fabrication limitations is inherently unavoidable. Research on the impact of disorder in quantum systems is an active area of study, e.g., [29–31]. Over the past few decades, the effects of disorder have also been extensively studied in the fields of cavity and waveguide QED [32–41]. These works demonstrated that disorder has significant impact on localization-delocalization and the quantum dynamics of the atomic excitations. However, the correlation of scattered photons in the presence of disorder remains relatively unexplored. Crucially, given that the correlation of scattered photons significantly depends on the nonlinearity, namely the level structure of the quantum emitters, this raises an intriguing question: can the system produce strongly correlated photons if the disorder in the level structure of quantum emitters is taken into account?

In this Letter, we address this question and give a positive answer by quantitatively studying the possibility of strong correlation events of scattered photons in a chain of N qubits coupled to a 1D waveguide. The strong correlation events studied in our Letter are photon antibunching (PA), perfect photon blockade (PPB), and nearly perfect photon blockade (NPPB) events, which have been extensively investigated across various physical systems [42–50]. For a resonant, weak classical input light, the transmission output does not generate antibunched photons when $N = 1$, while the reflection output always exhibits PPB due to the Pauli blockade. For $N = 2$, neither the transmission nor the reflection output produces antibunched photons. The presence of disorder does not change the possibility of these strong correlation events [see Fig. 1(b)].

When the chain contains multiple ($N > 2$) qubits, antibunched photons do not occur in the transmission output and only weakly antibunched photons occur in the reflection output. Notably, introducing disorder makes these strong correlation events possible. Especially, we show that the probability of NPPB events remains finite, in stark contrast to ordered chains where NPPB events are absent. The occurrence of NPPB events stems from the destructive interference of the photons' scattering path induced by the disorder.

*Contact author: zhenglili@jhun.edu.cn
†Contact author: xinyoulu@hust.edu.cn

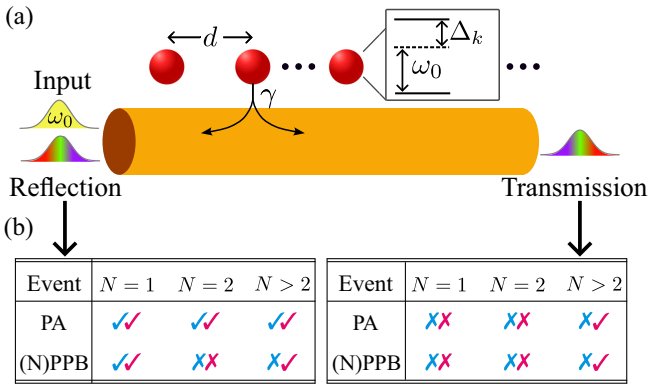

Event	$N=1$	$N=2$	$N>2$
PA	✓✓	✓✓	✓✓
(N)PPB	✓✓	✗✗	✗✓

Event	$N=1$	$N=2$	$N>2$
PA	✗✗	✗✗	✗✓
(N)PPB	✗✗	✗✗	✗✓

FIG. 1. (a) Schematics of a chain of qubits coupled to a 1D waveguide. The qubits have different transition frequencies denoted by $\omega_k = \omega_0 + \Delta_k$. The decay rate of each qubit is γ, and the qubits are uniformly spaced with distance d. For a weak classical input light with frequency ω_0, both the reflection and the transmission outputs can generate strongly correlated photons. (b) PA, PPB, and NPPB events for the reflection and transmission outputs. Here PPB (NPPB) corresponds to $N \leq 2 (N > 2)$. The corresponding event is possible (denoted by "51") or impossible ("55"). Blue (red) color denotes the events for systems without (with) disorder.

Furthermore, the probability of these strongly correlated photon events can be effectively increased by appropriately adjusting the system parameters. Specifically, increasing the chain size can enhance the probability of both PA and NPPB events in the transmission output, and the probability of NPPB events in the reflection output increases with disorder.

Model—Let us consider a right-propagating coherent pulse with frequency ω_0 (zero bandwidth) and strength α as input light interacting with a chain of N qubits with inhomogeneous transition frequency $\omega_m = \omega_0 + \Delta_m$ [see Fig. 1(a)]. The detunings of the qubits follow a normal distribution, i.e., $p(\Delta_1, \Delta_2, \ldots, \Delta_N) = \prod_{m=1}^{N} p(\Delta_m)$, with $p(\Delta_m) = \exp(-\Delta_m^2/2W^2)/\sqrt{2\pi W^2}$. We assume that the qubits only weakly deviate from the resonant frequency ω_0, with the condition $\omega_0/W \gg N$, such that the time evolution of the qubits can be described by the master equation $\dot{\rho} = -i[(H_{\rm eff} + H_d)\rho - \rho(H_{\rm eff}^\dagger + H_d)] + \sum_{mn} 2[\gamma_{\rm T}\Theta(m-n) + \gamma_{\rm R}\Theta(n-m) + \gamma_{\rm nw}\delta_{m,n}]\cos(|m-n|\varphi)\sigma_m\rho\sigma_n^\dagger$ [51,54]. Here $H_d = \sum_m \sqrt{\gamma_{\rm T}}\alpha(e^{im\varphi}\sigma_m^\dagger + {\rm H.c.})$, $\gamma_{\rm T}$ ($\gamma_{\rm R}$) is the individual decay rate of each qubit to transmission (reflection) waveguide mode, and $\gamma_{\rm nw}$ is the loss to nonwaveguide (nw) modes, $\varphi = \omega_0 d/c$, with d being the distance between adjacent qubits; $\Theta(x)$ denotes the Heaviside function. The non-Hermitian effective Hamiltonian is (in the rotated frame with respect to $H_0 = \sum_m \omega_0\sigma_m^\dagger\sigma_m$)

$$H_{\rm eff} = \sum_{m=1}^{N}\left(\Delta_m - \frac{i(\gamma_{\rm nw}+\gamma_{\rm T}+\gamma_{\rm R})}{2}\right)\sigma_m^\dagger\sigma_m - i\sum_{m>n}^{N}\left(\gamma_{\rm T}e^{i|m-n|\varphi}\sigma_m^\dagger\sigma_n + \gamma_{\rm R}e^{i|m-n|\varphi}\sigma_n^\dagger\sigma_m\right). \quad (1)$$

We consider $\gamma_{\rm nw} = 0$ and $\gamma_{\rm R} = \gamma_{\rm T} = \gamma/2$ in main text, discussing the impact of losses to nonwaveguide modes and the chirality in Supplemental Material [51]. We also discuss the effect of finite bandwidth of the input state. We show that the obtained results for a finite-bandwidth input show good agreements with those for zero-bandwidth input, provided that the bandwidth is an order of magnitude below the individual decay rate of qubit [51]. This validates the zero-bandwidth approximation considered in our Letter; and the requirement of such narrow bandwidth can be experimentally implemented in the state-of-the-art waveguide platforms [18,55,56]. Hereafter, we choose γ as the energy scale and set $\gamma = 1$ in our numerical calculations. We only consider $0 \leq \varphi \leq \pi/2$, due to the symmetry of this system.

The correlation of the emitted field is characterized by the zero-time second-order photon correlation function $g_\mu = \langle a_{\mu,\rm out}^{\dagger 2}(t)a_{\mu,\rm out}^2(t)\rangle/\langle a_{\mu,\rm out}^\dagger(t)a_{\mu,\rm out}(t)\rangle^2$, where $a_{\mu,\rm out}(t)$, with $\mu = {\rm T}$ (R) denoting the annihilation operator of the transmission (reflection) mode in the time domain. Utilizing the input-output formalism [57], the formal expressions of the correlations g_μ in the weak-drive limit, $\alpha \ll 1$, can be calculated as [51]

$$g_{\rm T} = \frac{|1 - 2i\langle\phi_+^1|\psi^1\rangle - \langle\phi_+^2|\psi^2\rangle|^2}{|1 - i\langle\phi_+^1|\psi^1\rangle|^4}, \quad g_{\rm R} = \frac{|\langle\phi_-^2|\psi^2\rangle|^2}{|\langle\phi_-^1|\psi^1\rangle|^4}. \quad (2)$$

Here $|\phi_\pm^1\rangle = \sqrt{1/2}\sum_m \exp(\pm im\varphi)\sigma_m^\dagger|G\rangle$ and $|\phi_\pm^2\rangle = \sum_{m>n}\exp[\pm i(m+n)\varphi]\sigma_m^\dagger\sigma_n^\dagger|G\rangle$, with $|G\rangle$ being the fully inverted ground state of qubits; $|\psi^1\rangle = -(H_{\rm eff}^{(1)})^{-1}H_+|G\rangle$ and $|\psi^2\rangle = -(H_{\rm eff}^{(2)})^{-1}H_+|\psi^1\rangle$ are, respectively, the single- and two-excitation component of the truncated steady-state solution for the qubit ensemble, with $H_+ = \sqrt{\gamma/2}\sum_m e^{im\varphi}\sigma_m^\dagger$. $H_{\rm eff}^{(1)}$ and $H_{\rm eff}^{(2)}$ are the single- and two-excitation sectors of Eq. (1). In the presence of disorder, the probability density functions of g_μ encode the full information of the photon correlations. The definition of the probability density function is given by $P(s) = \int_{-\infty}^{\infty}\cdots\int_{-\infty}^{\infty}\delta(g_\mu - s)p(\Delta_1, \ldots, \Delta_N){\rm d}\Delta_1\cdots{\rm d}\Delta_N$. The value of $P(s)$ ranges from 0 to infinity and is proportional to the probability of having a correlation function with value s. Especially, $P(\epsilon)$ with $\epsilon \to 0$ ($\epsilon = 0$) is proportional to the probability of an NPPB (PPB) event. We also define $\mathbb{P}(s<1) \coloneqq \int_0^1 P(s){\rm d}s$, which corresponds to the probability of the field being antibunched.

Photon correlations without system disorder—Photon correlations in the qubit chains, including the Markov property [24,58–62] and chirality [63], have been extensively studied. For the transmission output, when the qubits are strongly coupled ($\gamma_{\rm nw} = 0$) to the waveguide in a nonchiral configuration ($\gamma_{\rm R} = \gamma_{\rm T}$), a straightforward result is that $g_{\rm T}$ is always divergent regardless of the chain size N and distance d. The strong photon bunching occurs because

resonant qubits block the propagation of single photons from the input [64,65]; hence, the output field contains only multiphoton components. When the qubits are weakly coupled ($\gamma_{\rm nw} \gg \gamma_{\rm R} + \gamma_{\rm T}$) to the waveguide in a perfectly chiral configuration ($\gamma_{\rm R} = 0$), the photon statistics of the transmitted light evolve from Poissonian to antibunching and even bunching as the number of qubits increases [51], which is consistent with the results reported in [25]. For the reflection output, $g_{\rm R} = 0$ when a single qubit is coupled to the waveguide. This PPB occurs because a single qubit cannot be excited by two photons simultaneously [15]. When two qubits are coupled to the waveguide, the output light maintains coherent, i.e., $g_{\rm R} = 1$. When the chain contains $N > 2$ qubits, it is practically impossible to derive a closed-form expression for the correlation function. The numerical result for $g_{\rm R}$ as a function of N and φ is given in Fig. S4 of Supplemental Material [51]. The result shows that, for $N > 2$, the reflected photons exhibit weak bunching for φ within the range 0 to 0.25π and weak antibunching for φ within the range 0.3π to 0.5π.

Transmission photon correlations with system disorder—In the presence of disorder, the inhomogeneity in transition frequencies significantly modulates photon correlations in the transmission output. For a chain with a few qubits, we can derive an explicit expression of $g_{\rm T}$. For example, for a single-qubit system the correlation function is given by $g_{\rm T} = (1 + 4\Delta_1^2)^2/(16\Delta_1^4)$. In contrast to the divergent correlation obtained in a clean chain, $g_{\rm T}$ remains finite provided that the qubit is off resonant with the input (i.e., $\Delta_1 \neq 0$). However, one can readily show that $g_{\rm T} > 1$, which indicates that the transmission light is consistently bunched, thereby ruling out the possibility of PA and PPB. In other words, for a system with $N = 1$ it follows that $\mathbb{P}(s < 1) = P(0) = 0$. For an array with $N = 2$, the correlation function is given by

$$g_{\rm T} = \frac{q[(\Delta_1 + \Delta_2)^2(f_- - \cos\varphi) + p]}{\{64\Delta_1^4\Delta_2^4[1 + (\Delta_1 + \Delta_2)^2]\}}, \tag{3}$$

where $q = 8\Delta_1^2\Delta_2^2 + f_+ - \cos 2\varphi$ and $p = 8\Delta_1^2\Delta_2^2[1 + (\Delta_1 + \Delta_2)^2] + 4\Delta_1\Delta_2(\Delta_1 + \Delta_2)\sin 2\varphi$, with $f_\pm = 1 + 2\Delta_1^2 + 2\Delta_2^2 \pm 4\Delta_1\Delta_2\cos(2\varphi) - 2(\Delta_1 + \Delta_2)\sin(2\varphi)$. The correlation function has a minimum value $\min\{g_{\rm T}\} = 1$. Hence, the same conclusion applies to the two-qubit system, i.e., $\mathbb{P}(s < 1) = 0$ and $P(0) = 0$.

When the chain contains more than two qubits, an explicit expression of the correlation function becomes too complex to work out $\mathbb{P}(s < 1)$ analytically [51]. In Figs. 2(a) and 2(b), we present the numerical results of $\mathbb{P}(s < 1)$ under various phases, chain sizes, and disorder strengths. In contrast to the few-qubit array, these results show that antibunched photons can occur in the transmission output. Notably, in the intermediate-disorder regime [$W \sim \mathcal{O}(1)$], $\mathbb{P}(s < 1)$ attains its maximum value when the array is highly dense ($\varphi \ll 1$) and the chain size is

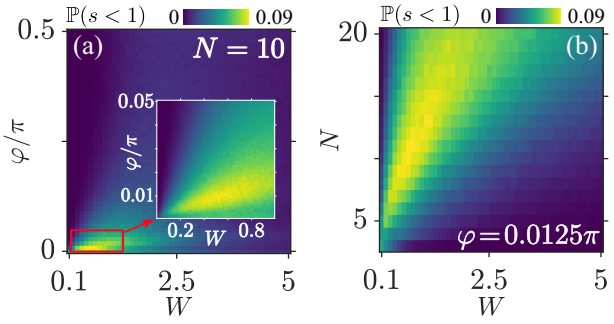

FIG. 2. Correlation statistics of the transmission output. Probability of PA versus φ and W in (a), and versus N and W in (b). Inset in (a) displays the close-up of (a). $N = 10$ in (a). In (b), $\varphi = 0.0125\pi$, corresponding to the position where $\mathbb{P}(s < 1)$ in (a) reaches its maximum value. In all plots, the results are obtained from Monte Carlo integration. The numerical details are discussed in Supplemental Material [51].

appropriately taken. Such a requirement from a deeply subwavelength qubit array can be relaxed by the periodicity $\varphi \to \varphi + 2\pi$ of the system [51]. Moreover, the deeply subwavelength qubit distance is experimentally feasible in the state-of-the-art superconducting platforms [20] so that the condition $\varphi \ll 1$ can also be experimentally implemented. For a sparse array, $\mathbb{P}(s < 1)$ rapidly decreases with either an increase or a decrease in the disorder strength. In the weak-disorder limit $W \ll 1$, a single photon has a low probability of propagating through the chain, resulting in a low probability of PA. In the strong-disorder limit $W \gg 1$, the long-range interaction mediated by photons is largely quenched; consequently, the probability of PA decreases as disorder becomes too strong [51].

Regarding the possibility of NPPB events, we first present the probability density function for a system with $N = 3$ and $\varphi/\pi = 0.04$ in Fig. 3(a). Our results indicate that $P(s)$ saturates to a constant value for $s \ll 1$, implying that $P(s \to 0) \neq 0$. This behavior of $P(s)$ is attributed to the existence of specific detuning values $\{\Delta_1, \Delta_2, \Delta_3\}$ that satisfy the NPPB condition $g_{\rm T} = \varepsilon$ [see the inset of Fig. 3(a)], where ε can be arbitrarily close to 0 [51]. According to scattering theory [27], these NPPB events stem from the nearly completely destructive interference of single-photon scattering paths with probability amplitude $\langle\phi_+^1|\psi^1\rangle$, the two-photon scattering paths with probability amplitude $\langle\phi_+^2|\psi^2\rangle$, and the free propagation paths with probability amplitude 1. These scattering paths are further determined by the transition paths that are governed by the non-Hermitian effective Hamiltonian Eq. (1). A detailed discussion of these destructive effects is provided in [51]. Considering such asymptotic behavior of $P(s)$, hereafter, we adopt $P(10^{-3})$ as the representative value of the probability density function for an NPPB event. In Figs. 3(c) and 3(d), we present $P(10^{-3})$ for different system parameters. Our results show that NPPB events can occur, provided that $\varphi \neq 0$. In the Dicke limit $\varphi = 0$,

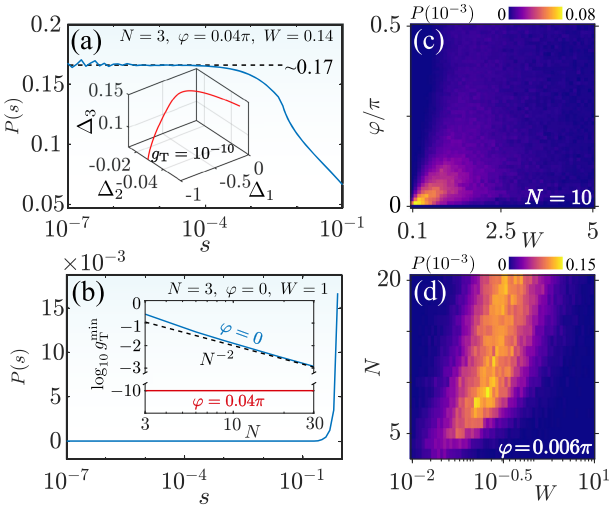

FIG. 3. Correlation statistics of the transmission output. (a,b) Probability density functions. The chosen parameters are $\{N=3, \varphi=0.04\pi, W=0.14\}$ in (a) and $\{N=3, \varphi=0, W=1\}$ in (b). Inset of (a) shows the solutions $\{\Delta_1, \Delta_2, \Delta_3\}$ that satisfy $g_T = 10^{-10}$. The solutions are constrained to $|\Delta_j| \leq 1$. Inset of (b) shows $g_T^{\min}$, corresponding to the minimum value of g_T, for $\varphi = 0$ (blue line) and for $\varphi = 0.04\pi$ (orange line) with respect to chain size, and the dashed line is the numerical fit N^{-2}. (c,d) $P(10^{-3})$ versus φ and W in (c), and versus N and W in (d). $N = 10$ in (c). In (d), $\varphi = 0.006\pi$, corresponding to the position where $P(10^{-3})$ in (c) reaches its maximum value.

however, we find $P(10^{-3}) = 0$ for relatively small chain sizes [see Fig. 3(b)]. In this case, $P(10^{-3})$ vanishes because, unlike the systems with $\varphi \neq 0$ where g_T can be arbitrarily close to 0, the correlation function for $\varphi = 0$ can only attain a minimal value that scales as N^{-2} with the chain size [see the inset of Fig. 3(b)]. This indicates that $P(\epsilon) = 0$ for $\epsilon \lesssim N^{-2}$.

Our results shown in Figs. 2 and 3 demonstrate that both $\mathbb{P}(s<1)$ and $P(10^{-3})$ can attain their optimal (maximum) values when system parameters are suitably tuned. We subsequently investigate how these optimal values depend on the system parameters. As shown in Fig. 4(a), the maximum values of $\mathbb{P}(s<1)$ and $P(10^{-3})$ exhibit power-law scaling with the number N of qubits according to $(1-0.97N^{-1/40})$ and $0.04N^{1/2}$, respectively. In addition to power-law scaling, the dependence of these optimal values on W and φ exhibits both similar and distinctive features. Specifically, as the number of qubits increases, the optimal values of $\mathbb{P}(s<1)$ and $P(10^{-3})$ are reached at lower values of φ; however, achieving the maximum $\mathbb{P}(s<1)$ requires a stronger disorder strength, whereas the maximum $P(10^{-3})$ is obtained when the disorder strength is around 0.15 [see Figs. 4(b) and 4(c)].

Reflection photon correlations with system disorder—One can expect that correlations in the reflection output to exhibit behaviors distinct from those obtained in the transmission output, since reflected photons necessarily

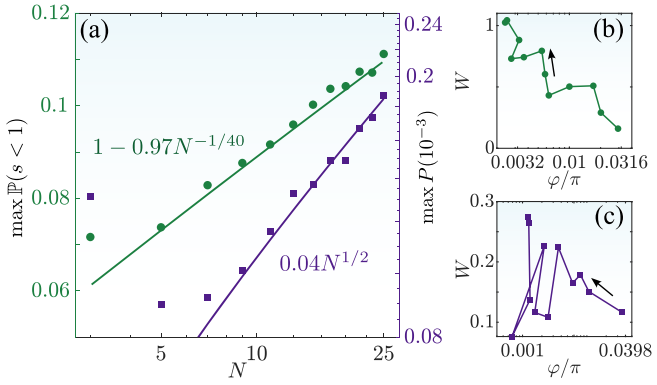

FIG. 4. Correlation statistics of the transmission output. (a) The maximum values of $\mathbb{P}(s<1)$ and $P(10^{-3})$ versus N. Green circles (purple squares) display the maximum values of $\mathbb{P}(s<1)$ $[P(10^{-3})]$ versus N. Green and purple solid lines are the numerical fits of $1-0.97N^{-1/40}$ and $0.04N^{1/2}$, respectively. (b) and (c) display W and φ, respectively, where $\mathbb{P}(s<1)$ and $P(10^{-3})$ reach their maximum values. Black arrows point in the direction of increasing N. Inset of (c) displays the close-up of (c).

interact with the qubits, whereas transmitted photons can pass through the waveguide without interaction. In the presence of disorder, it is evident that $g_R = 0$ for $N = 1$, implying that only PPB events occur. For a two-qubit chain, the correlation function is given by $g_R = |[-i + i\exp(2i\varphi) + 2\Delta_1 + 2\Delta_2][\exp(2i\varphi) + (2\Delta_1 - i)(2\Delta_2 - i)]/\{[\Delta_1 + \Delta_2 - i][2\Delta_2 - i + \exp(2i\varphi)(2\Delta_1 + i)]^2\}|^2$. Based on this explicit expression, in Supplemental Material [51] we show analytically and numerically that

$$\mathbb{P}(s<1) \geq \frac{2}{3}, \qquad P(0) = 0. \tag{4}$$

This result reveals two features: (i) introducing disorder enables PA events, with a probability exceeding 1/2, indicating that the output light is more likely to be antibunched; and (ii) despite the possibility of PA, the two-qubit system rules out the possibility of PPB, due to the absence of destructive interference of two-photon scattering paths. In fact, only strong PA can occur, provided that one qubit is far off resonant while the other remains nearly resonant. In this case, the two-photon scattering probability amplitude $\langle \phi_-^2 | \psi^2 \rangle$ is near zero, due to a large detuning, $|\Delta_1 + \Delta_2| \gg 1$, between the two-excitation state of the qubits and the two-photon state of the input; meanwhile, the single-photon scattering probability amplitude $\langle \phi_-^1 | \psi^1 \rangle$ is near unity, since the nearly resonant qubit blocks the transmission of single photons from the input. However, the PPB events can never occur, since $\langle \phi_-^2 | \psi^2 \rangle$ can never be exactly zero, due to the finite detuning of the far off-resonant qubit.

For a chain with $N > 2$, the behavior of $\mathbb{P}(s<1)$ is distinct from those obtained in chains with fewer qubits. In Figs. 5(a) and 5(b), we present the results of $\mathbb{P}(s<1)$ for

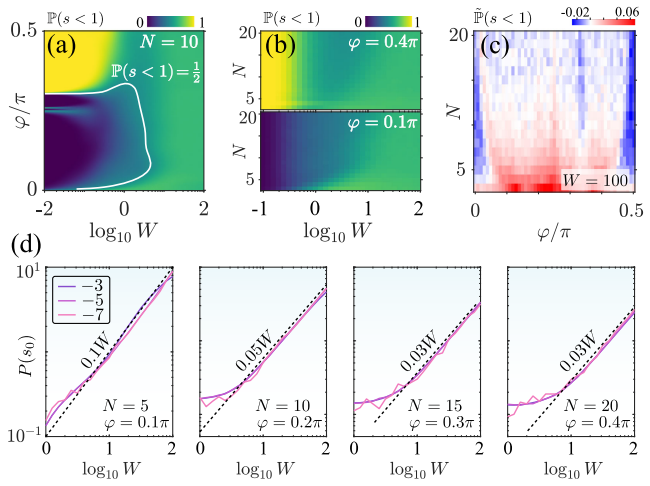

FIG. 5. Correlation statistics of the reflection output. $\mathbb{P}(s<1)$ versus φ and W in (a), and versus N and W in (b). The white solid curve in (a) denotes the regime where $\mathbb{P}(s<1)=1/2$. $N=10$ in (a). $\varphi=0.4\pi$ ($\varphi=0.1\pi$) in the top (bottom) of (b). (c) $\tilde{\mathbb{P}}(s<1)$ for different chain sizes and phases, with $\tilde{\mathbb{P}}(s<1)=\mathbb{P}(s<1)-2/3$. $W=100$ in (c). (d) $P(10^{-\mu})$ versus disorder strength. Solid lines in different colors correspond to different values of μ, with $\mu=-3,-5,-7$. Dashed lines are the numerical slopes. In (d), we only consider the contributions from noninteracting transition paths, whose validation is discussed in [51]. Results are obtained from 10^{10} disorder realizations.

different system parameters. Our results reveal that, for $W \ll 1$, the system exhibits a high (low) probability of PA when $0.3\pi<\varphi<0.5\pi$ ($0<\varphi<0.25\pi$). As disorder strength increases, the probability of PA decreases (increases) when $0.3\pi<\varphi<0.5\pi$ ($0<\varphi<0.25\pi$). In the strong-disorder regime, $\mathbb{P}(s<1)$, especially for large chain sizes, saturates at a value close to $2/3$ [see Fig. 5(c)]. This value corresponds to the probability of PA for the two-qubit system with $\varphi=0$ [51]. Regarding the probability of NPPB, its value increases and follows a power-law scaling with disorder strength when $W \gg 1$ [see Fig. 5(d)]. This is in contrast to the results of the transmission output, where $P(10^{-3})$ rapidly decreases when disorder becomes too strong. We show in Supplemental Material that [51] the enhancement of the probability of NPPB events in the reflection output stems from the fact that NPPB events involve solely the nearly completely destructive interference of two-photon noninteracting scattering paths.

Conclusion—In summary, we have investigated the possibility of generating repulsively correlated photons in a chain of qubits coupled to a 1D waveguide. We found that, in the presence of disorder, it is possible to produce antibunched and nearly perfect blockaded photons, provided that the system parameters N, φ, and W are suitably chosen. Furthermore, we demonstrate that the interplay among these parameters can significantly modulate the probability of strongly correlated photon events. Notably, our results reveal that the probabilities of PA and NPPB increase with the number of qubits according to a power-law scaling, while the probability of NPPB exhibits a power-law scaling with disorder strength. Our findings not only reveal the critical role of disorder in enabling strong photon correlations but also pave the way for disorder-engineered strongly correlated photons and potential single-photon sources.

Acknowledgments—We sincerely thank Professor Francesco Ciccarello for his valuable suggestions and insightful comments, which have greatly improved this work. We also thank Zhi-Guang Lu for his valuable suggestions. X.-Y. L. is supported by the National Science Fund for Distinguished Young Scholars of China (Grant No. 12425502), the Innovation Program for Quantum Science and Technology (Grant No. 2024ZD0301000), the National Key Research and Development Program of China (Grant No. 2021YFA1400700), and the Fundamental Research Funds for the Central Universities (Grant No. 2024BRA001). F. N. is supported in part by the Japan Science and Technology Agency (JST) [via the CREST Quantum Frontiers program Grant No. JPMJCR24I2, the Quantum Leap Flagship Program (Q-LEAP), and the Moonshot R&D Grant No. JPMJMS2061], and the Office of Naval Research (ONR) Global (via Grant No. N62909-23-1-2074).

Data availability—The data that support the findings of this Letter are not publicly available. The data are available from the authors upon reasonable request.

[1] H. J. Kimble, The quantum internet, Nature (London) **453**, 1023 (2008).
[2] X. Lu, Q. Li, D. A. Westly, G. Moille, A. Singh, V. Anant, and K. Srinivasan, Chip-integrated visible–telecom entangled photon pair source for quantum communication, Nat. Phys. **15**, 373 (2019).
[3] L. Zhou, Z. R. Gong, Y.-x. Liu, C. P. Sun, and F. Nori, Controllable scattering of a single photon inside a one-dimensional resonator waveguide, Phys. Rev. Lett. **101**, 100501 (2008).
[4] E. Knill, R. Laflamme, and G. J. Milburn, A scheme for efficient quantum computation with linear optics, Nature (London) **409**, 46 (2001).
[5] J. L. O'Brien, Optical quantum computing, Science **318**, 1567 (2007).
[6] P. Kok, W. J. Munro, K. Nemoto, T. C. Ralph, J. P. Dowling, and G. J. Milburn, Linear optical quantum computing with photonic qubits, Rev. Mod. Phys. **79**, 135 (2007).
[7] I. Carusotto and C. Ciuti, Quantum fluids of light, Rev. Mod. Phys. **85**, 299 (2013).
[8] D. Roy, C. M. Wilson, and O. Firstenberg, Colloquium: Strongly interacting photons in one-dimensional continuum, Rev. Mod. Phys. **89**, 021001 (2017).
[9] K. M. Birnbaum, A. Boca, R. Miller, A. D. Boozer, T. E. Northup, and H. J. Kimble, Photon blockade in an optical

cavity with one trapped atom, Nature (London) **436**, 87 (2005).
[10] H. Walther, B. T. Varcoe, B.-G. Englert, and T. Becker, Cavity quantum electrodynamics, Rep. Prog. Phys. **69**, 1325 (2006).
[11] N. Lambert, Y.-N. Chen, and F. Nori, Unified single-photon and single-electron counting statistics: From cavity QED to electron transport, Phys. Rev. A **82**, 063840 (2010).
[12] A. Reiserer and G. Rempe, Cavity-based quantum networks with single atoms and optical photons, Rev. Mod. Phys. **87**, 1379 (2015).
[13] D. Chang, J. Douglas, A. González-Tudela, C.-L. Hung, and H. J. Kimble, Colloquium: Quantum matter built from nanoscopic lattices of atoms and photons, Rev. Mod. Phys. **90**, 031002 (2018).
[14] M. Reitz, C. Sommer, and C. Genes, Cooperative quantum phenomena in light-matter platforms, PRX Quantum **3**, 010201 (2022).
[15] A. S. Sheremet, M. I. Petrov, I. V. Iorsh, A. V. Poshakinskiy, and A. N. Poddubny, Waveguide quantum electrodynamics: Collective radiance and photon-photon correlations, Rev. Mod. Phys. **95**, 015002 (2023).
[16] E. Vetsch, D. Reitz, G. Sagué, R. Schmidt, S. T. Dawkins, and A. Rauschenbeutel, Optical interface created by laser-cooled atoms trapped in the evanescent field surrounding an optical nanofiber, Phys. Rev. Lett. **104**, 203603 (2010).
[17] M. A. Versteegh, M. E. Reimer, K. D. Jöns, D. Dalacu, P. J. Poole, A. Gulinatti, A. Giudice, and V. Zwiller, Observation of strongly entangled photon pairs from a nanowire quantum dot, Nat. Commun. **5**, 5298 (2014).
[18] S. Faez, P. Türschmann, H. R. Haakh, S. Götzinger, and V. Sandoghdar, Coherent interaction of light and single molecules in a dielectric nanoguide, Phys. Rev. Lett. **113**, 213601 (2014).
[19] A. Sipahigil, R. E. Evans, D. D. Sukachev, M. J. Burek, J. Borregaard, M. K. Bhaskar, C. T. Nguyen, J. L. Pacheco, H. A. Atikian, C. Meuwly *et al.*, An integrated diamond nanophotonics platform for quantum-optical networks, Science **354**, 847 (2016).
[20] J. D. Brehm, A. N. Poddubny, A. Stehli, T. Wolz, H. Rotzinger, and A. V. Ustinov, Waveguide bandgap engineering with an array of superconducting qubits, npj Quantum Mater. **6**, 10 (2021).
[21] L. Zhou, H. Dong, Y.-x. Liu, C. P. Sun, and F. Nori, Quantum supercavity with atomic mirrors, Phys. Rev. A **78**, 063827 (2008).
[22] J. R. Johansson, G. Johansson, C. M. Wilson, and F. Nori, Dynamical Casimir effect in a superconducting coplanar waveguide, Phys. Rev. Lett. **103**, 147003 (2009).
[23] J.-Q. Liao, Z. R. Gong, L. Zhou, Y.-x. Liu, C. P. Sun, and F. Nori, Controlling the transport of single photons by tuning the frequency of either one or two cavities in an array of coupled cavities, Phys. Rev. A **81**, 042304 (2010).
[24] T. Shi, D. E. Chang, and J. I. Cirac, Multiphoton-scattering theory and generalized master equations, Phys. Rev. A **92**, 053834 (2015).
[25] A. S. Prasad, J. Hinney, S. Mahmoodian, K. Hammerer, S. Rind, P. Schneeweiss, A. S. Sørensen, J. Volz, and A. Rauschenbeutel, Correlating photons using the collective nonlinear response of atoms weakly coupled to an optical mode, Nat. Photonics **14**, 719 (2020).
[26] H. Le Jeannic, A. Tiranov, J. Carolan, T. Ramos, Y. Wang, M. H. Appel, S. Scholz, A. D. Wieck, A. Ludwig, N. Rotenberg *et al.*, Dynamical photon–photon interaction mediated by a quantum emitter, Nat. Phys. **18**, 1191 (2022).
[27] Z.-G. Lu, C. Shang, Y. Wu, and X.-Y. Lü, Analytical approach to higher-order correlation functions in U(1) symmetric systems, Phys. Rev. A **108**, 053703 (2023).
[28] M. Tečer, M. Di Liberto, P. Silvi, S. Montangero, F. Romanato, and G. Calajó, Strongly interacting photons in 2D waveguide QED, Phys. Rev. Lett. **132**, 163602 (2024).
[29] E. Abrahams, P. W. Anderson, D. C. Licciardello, and T. V. Ramakrishnan, Scaling theory of localization: Absence of quantum diffusion in two dimensions, Phys. Rev. Lett. **42**, 673 (1979).
[30] F. Evers and A. D. Mirlin, Anderson transitions, Rev. Mod. Phys. **80**, 1355 (2008).
[31] D. A. Abanin, E. Altman, I. Bloch, and M. Serbyn, Colloquium: Many-body localization, thermalization, and entanglement, Rev. Mod. Phys. **91**, 021001 (2019).
[32] E. Akkermans, A. Gero, and R. Kaiser, Photon localization and Dicke superradiance in atomic gases, Phys. Rev. Lett. **101**, 103602 (2008).
[33] H. H. Jen, Disorder-assisted excitation localization in chirally coupled quantum emitters, Phys. Rev. A **102**, 043525 (2020).
[34] N. Fayard, L. Henriet, A. Asenjo-Garcia, and D. E. Chang, Many-body localization in waveguide quantum electrodynamics, Phys. Rev. Res. **3**, 033233 (2021).
[35] C. Sommer, M. Reitz, F. Mineo, and C. Genes, Molecular polaritonics in dense mesoscopic disordered ensembles, Phys. Rev. Res. **3**, 033141 (2021).
[36] G. Fedorovich, D. Kornovan, A. Poddubny, and M. Petrov, Chirality-driven delocalization in disordered waveguide-coupled quantum arrays, Phys. Rev. A **106**, 043723 (2022).
[37] N. Sauerwein, F. Orsi, P. Uhrich, S. Bandyopadhyay, F. Mattiotti, T. Cantat-Moltrecht, G. Pupillo, P. Hauke, and J.-P. Brantut, Engineering random spin models with atoms in a high-finesse cavity, Nat. Phys. **19**, 1128 (2023).
[38] V. Viggiano, R. Bachelard, F. D. Cunden, P. Facchi, R. Kaiser, S. Pascazio, and F. V. Pepe, Cooperative photon emission rates in random atomic clouds, Phys. Rev. A **108**, 063701 (2023).
[39] M. Lei, R. Fukumori, J. Rochman, B. Zhu, M. Endres, J. Choi, and A. Faraon, Many-body cavity quantum electrodynamics with driven inhomogeneous emitters, Nature (London) **617**, 271 (2023).
[40] F. Mattiotti, J. Dubail, D. Hagenmüller, J. Schachenmayer, J.-P. Brantut, and G. Pupillo, Multifractality in the interacting disordered Tavis-Cummings model, Phys. Rev. B **109**, 064202 (2024).
[41] N. O. Gjonbalaj, S. Ostermann, and S. F. Yelin, Modifying cooperative decay via disorder in atom arrays, Phys. Rev. A **109**, 013720 (2024).
[42] A. Faraon, I. Fushman, D. Englund, N. Stoltz, P. Petroff, and J. Vučković, Coherent generation of non-classical light on a chip via photon-induced tunnelling and blockade, Nat. Phys. **4**, 859 (2008).

[43] T. C. H. Liew and V. Savona, Single photons from coupled quantum modes, Phys. Rev. Lett. **104**, 183601 (2010).
[44] C. Lang, D. Bozyigit, C. Eichler, L. Steffen, J. M. Fink, A. A. Abdumalikov, M. Baur, S. Filipp, M. P. da Silva, A. Blais, and A. Wallraff, Observation of resonant photon blockade at microwave frequencies using correlation function measurements, Phys. Rev. Lett. **106**, 243601 (2011).
[45] J.-Q. Liao and F. Nori, Photon blockade in quadratically coupled optomechanical systems, Phys. Rev. A **88**, 023853 (2013).
[46] A. Miranowicz, J. c. v. Bajer, M. Paprzycka, Y.-x. Liu, A. M. Zagoskin, and F. Nori, State-dependent photon blockade via quantum-reservoir engineering, Phys. Rev. A **90**, 033831 (2014).
[47] H. Flayac and V. Savona, Unconventional photon blockade, Phys. Rev. A **96**, 053810 (2017).
[48] R. Huang, A. Miranowicz, J.-Q. Liao, F. Nori, and H. Jing, Nonreciprocal photon blockade, Phys. Rev. Lett. **121**, 153601 (2018).
[49] R. Huang, Ş K. özdemir, J.-Q. Liao, F. Minganti, L.-M. Kuang, F. Nori, and H. Jing, Exceptional photon blockade: Engineering photon blockade with chiral exceptional points, Laser Photonics Rev. **16**, 2100430 (2022).
[50] Z.-G. Lu, Y. Wu, and X.-Y. Lü, Chiral interaction induced near-perfect photon blockade, Phys. Rev. Lett. **134**, 013602 (2025).
[51] See Supplemental Material at http://link.aps.org/supplemental/10.1103/mldt-d59tfor the derivation of the second-order correlation function and the detailed calculation of the probability density function, which includes Refs. [52,53].
[52] A. Asenjo-Garcia, M. Moreno-Cardoner, A. Albrecht, H. J. Kimble, and D. E. Chang, Exponential improvement in photon storage fidelities using subradiance and "selective radiance" in atomic arrays, Phys. Rev. X **7**, 031024 (2017).
[53] Y. Wang, W. Verstraelen, B. Zhang, T. C. H. Liew, and Y. D. Chong, Giant enhancement of unconventional photon blockade in a dimer chain, Phys. Rev. Lett. **127**, 240402 (2021).
[54] D. A. Lidar, Lecture notes on the theory of open quantum systems, arXiv:1902.00967.
[55] B. Kuyken, T. Ideguchi, S. Holzner, M. Yan, T. W. Hänsch, J. Van Campenhout, P. Verheyen, S. Coen, F. Leo, R. Baets *et al.*, An octave-spanning mid-infrared frequency comb generated in a silicon nanophotonic wire waveguide, Nat. Commun. **6**, 6310 (2015).
[56] Z. Bao, Y. Li, Z. Wang, J. Wang, J. Yang, H. Xiong, Y. Song, Y. Wu, H. Zhang, and L. Duan, A cryogenic on-chip microwave pulse generator for large-scale superconducting quantum computing, Nat. Commun. **15**, 5958 (2024).
[57] T. Caneva, M. T. Manzoni, T. Shi, J. S. Douglas, J. I. Cirac, and D. E. Chang, Quantum dynamics of propagating photons with strong interactions: A generalized input–output formalism, New J. Phys. **17**, 113001 (2015).
[58] H. Zheng and H. U. Baranger, Persistent quantum beats and long-distance entanglement from waveguide-mediated interactions, Phys. Rev. Lett. **110**, 113601 (2013).
[59] Y.-L. L. Fang, H. Zheng, and H. U. Baranger, One-dimensional waveguide coupled to multiple qubits: Photon-photon correlations, Eur. Phys. J. Quantum Technol. **1**, 3 (2014).
[60] Y.-L. L. Fang and H. U. Baranger, Waveguide QED: Power spectra and correlations of two photons scattered off multiple distant qubits and a mirror, Phys. Rev. A **91**, 053845 (2015).
[61] Y.-L. L. Fang, F. Ciccarello, and H. U. Baranger, Non-Markovian dynamics of a qubit due to single-photon scattering in a waveguide, New J. Phys. **20**, 043035 (2018).
[62] P. R. Berman, Theory of two atoms in a chiral waveguide, Phys. Rev. A **101**, 013830 (2020).
[63] S. Mahmoodian, M. Čepulkovskis, S. Das, P. Lodahl, K. Hammerer, and A. S. Sørensen, Strongly correlated photon transport in waveguide quantum electrodynamics with weakly coupled emitters, Phys. Rev. Lett. **121**, 143601 (2018).
[64] D. E. Chang, L. Jiang, A. Gorshkov, and H. J. Kimble, Cavity QED with atomic mirrors, New J. Phys. **14**, 063003 (2012).
[65] L. Leonforte, A. Carollo, and F. Ciccarello, Vacancy-like dressed states in topological waveguide QED, Phys. Rev. Lett. **126**, 063601 (2021).